Genetica
DOI 10.1007/s10709-013-9727-4

Taxonomic and population genetic re-interpretation of two color morphs of the decollate snail, *Rumina decollata* (Mollusca, Pulmonata) in southern France

Vanya Prévot · Kurt Jordaens · Natalie Van Houtte · Gontran Sonet · Kenny Janssens · Rita Castilho · Thierry Backeljau

Received: 25 March 2013 / Accepted: 16 July 2013

Abstract The hermaphroditic terrestrial snail *Rumina decollata* has a mixed breeding system with a high prevalence of self-fertilization. In the Montpellier area (France), the species is represented by a dark and a light color morph. Based on allozyme data, both morphs have been reported as single, homozygous multilocus genotypes (MLG), differing at 13 out of 26 loci, but still showing occasional hybridization. Recent DNA sequence data suggest that each morph is a different phylogenetic species. In order to further evaluate this new taxonomic interpretation, the present contribution explores to what extent populations or color morphs indeed consist of single or few MLG. As such it is shown that both morphs are not single, homozygous MLG, but instead reveal a considerable amount of allelic variation and substantial numbers of heterozygous microsatellite genotypes. This suggests that outcrossing may be more prevalent than previously reported. Nevertheless, both morphs maintain a diagnostic multimarker differentiation in the presence of outcrossing in sympatric conditions, implying that they may be interpreted as species under the biological species concept. Finally, our data challenge the idea that simultaneous hermaphrodites should be either strict selfers or strict outcrossers.

Keywords Allozymes · Microsatellites · DNA sequences · Color polymorphism · Population genetics · Self-fertilization

Electronic supplementary material The online version of this article (doi:10.1007/s10709-013-9727-4) contains supplementary material, which is available to authorized users.

V. Prévot (✉) · K. Janssens · T. Backeljau
Department of Invertebrates and JEMU, Royal Belgian Institute of Natural Sciences, Rue Vautier 29, 1000 Brussels, Belgium
e-mail: vanya.prevot@naturalsciences.be

V. Prévot
Laboratoire d'Evolution Biologique et Ecologie, Université Libre de Bruxelles (ULB), Avenue F.D. Roosevelt 50, 1050 Brussels, Belgium

K. Jordaens · N. Van Houtte · T. Backeljau
Evolutionary Ecology Group, University of Antwerp, Groenenborgerlaan 171, 2020 Antwerp, Belgium

K. Jordaens · G. Sonet
Joint Experimental Molecular Unit (JEMU), Royal Museum for Central Africa, Leuvensesteenweg 13, 3080 Tervuren, Belgium

R. Castilho
Centro de Ciências do Mar (CCMAR), Universidade do Algarve, Campus de Gambelas, 8005-139 Faro, Portugal

Introduction

Mixed breeding systems in hermaphroditic gastropods pose challenging taxonomic problems because frequent self-fertilization may promote genotypic and phenotypic differentiation by fixation of alternative alleles at various nuclear gene loci (e.g. Backeljau et al. 1997; Jordaens et al. 2000). Insofar these loci code for traits that are used for taxonomic purposes (e.g. allozyme electromorphs, morphological characters with Mendelian inheritance, …), the resulting multilocus genotypes (MLG) may have divergent phenotypes that can easily be regarded as different species (e.g. Geenen et al. 2006).

A particularly illustrative case in which a mixed breeding system may have confused taxonomic interpretations is the decollate pulmonate land snail *Rumina decollata* (Linnaeus, 1758; Stylommatophora: Subulinidae), a

Published online: 26 July 2013

common and widespread taxon in the Mediterranean region. Although *R. decollata* regularly displays mating behavior and hence is supposed to outcross (Batts 1957; Dundee 1986), the species also seems to frequently self-fertilize (e.g. Selander and Kaufman 1973; Selander et al. 1974). As a consequence, *R. decollata* appears to be a complex of >30 MLG defined by homozygous allelic combinations at 25–26 allozyme loci and body color (Selander and Ochman 1983). Populations usually consist of single, or very few, MLG and spatial genetic structuring is very strong: groups of animals living only 5 m apart may have a different genetic composition, suggesting that migration must be very limited (Selander and Hudson 1976; Selander and Ochman 1983).

Two MLG of *R. decollata* that differ at 13 of 26 allozyme loci co-occur in the Montpellier area (southern France; Selander and Hudson 1976). One MLG has a black body with a dull olive-gray foot (= dark strain), while the other MLG has a light gray body with a medio-dorsal black line and a pale yellowish foot (= light strain; Fig. 1). Both MLG have different life-history characteristics: (1) light specimens tend to live in more exposed habitats, while the dark specimens occur in more mesic habitats, (2) dark specimens are less active than light ones, (3) light specimens have a faster embryonic and post-hatching development, so that they start reproducing at a much younger age than dark specimens and (4) the number and total weight of eggs laid per day are larger in dark specimens (Selander and Hudson 1976; Selander and Ochman 1983).

Despite their allozymic, morphological and life history differences, the two MLG occasionally hybridize and produce "intermediate" body color phenotypes showing a mixture of allozyme alleles typical for the light or dark morph (Selander and Hudson 1976). Unfortunately, except for the presumption that fitness is reduced in these hybrids, no further information about hybrid lifetime reproductive success was provided by Selander and Hudson (1976). Yet, despite this occasional hybridization, populations of *R. decollata* show little, if any, MLG diversity, because different MLG have different reproductive characteristics (fecundity, reproductive period, …) so that at the population level eventually only one or few MLG will predominate (Selander and Ochman 1983).

Until recently *R. decollata* was treated as a single species. Yet, using DNA sequence data Prévot et al. (2013) assessed whether the phenotypic differentiation in *R. decollata* correlated with historical divergences that can be interpreted under a phylogenetic species concept. As such, Prévot et al. (2013) found that the two color morphs in Montpellier represent two highly divergent clades that group all the dark (clade A) and all the light animals (clade Eb), and that both were considered as phylogenetic species. Both clades have overlapping geographic distributions, particularly in southern France, where the light and dark morphs can locally co-occur (Prévot et al. 2013).

Obviously, the new taxonomic interpretation of *R. decollata* calls for a re-assessment of the earlier population genetic analyses of this species. Therefore, we re-analyzed the population genetic structure of the two color morphs of *R. decollata* in the Montpellier region. To this end we combined allozyme electrophoresis, DNA microsatellite genotyping and DNA nucleotide sequencing to (1) test the allozyme-based observation that most populations consist of single or few MLG and that each color morph is a single MLG (2) assess the amount of genetic differentiation or eventual gene flow between populations or color morphs using highly polymorphic microsatellite loci, and (3) discuss the taxonomic interpretation of the two color morphs as phylogenetic and/or biological species. Because the taxonomic re-interpretation of the *R. decollata* color morphs is not yet nomenclaturally formalized, we will continue to apply the name *R. decollata* to both of them.

Materials and methods

Sampling

Rumina decollata was collected in May 2008 by hand-picking from four of five localities sampled by Selander and Hudson (1976) and Selander and Ochman (1983) in the

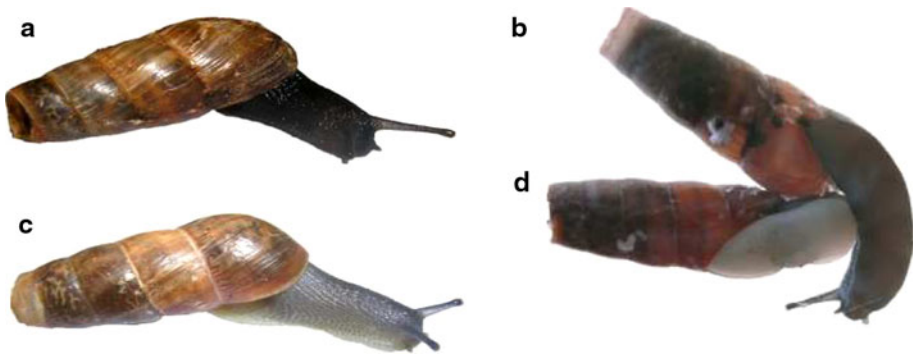

Fig. 1 The *dark* (**a**, **b**) and *light* (**c**, **d**) *color* morphs *R. decollata*

city of Montpellier, southern France (Botanical Garden, Lycée de Joffre, Protestant Cemetery, and Boulevard des Arceaux; Table 1, Fig. 2). One additional locality was sampled in the center of Montpellier (= "Montpellier Spot 1"; FmtS; Table 1, Fig. 2). Two sites were sampled in the Botanical garden: FmtB1, i.e. in the garden itself, and FmtB2, which was a plant container near the entrance of the Botanical garden. Selander and Hudson (1976) collected no <2 280 specimens from 24 colonies at Boulevard des Arceaux. We, in contrast, found only two small colonies at this site (FmtA1 and FmtA2). A total of 98 specimens were collected from these seven sites. After sampling, animals were stored at −80 °C. The material comprised 34 specimens of the dark morph (= "dark specimens"), 63 specimens of the light morph (= "light specimens") and one intermediate (dark body and light foot; = "intermediate specimen"). All specimens were photographed and the color of the foot (olive-gray or pale yellow) and body (black or gray with a black line on the back) was recorded.

Allozymes

As our attempts to apply starch gel electrophoresis yielded very poor results, we used polyacrylamide gel electrophoresis (PAGE) instead. This was not expected to produce fundamentally different results (Geenen et al. 2003).

The digestive gland of 96 individuals (31 dark, 63 light and 1 intermediate) was dissected to prepare tissue homogenates for vertical PAGE as outlined in Backeljau (1987). Variation was assessed at six enzyme systems. A continuous Tris/Citric acid (pH 8.0) buffer system was used to resolve isocitrate dehydrogenase (*Idh*, EC 1.1.1.42), leucine amino peptidase (*Lap*, EC 3.4.1.1), malate dehydrogenase (*Mdh*, EC 1.1.1.37), phosphogluconate dehydrogenase (*Pgd*, E.C. 1.1.1.43) and glucose-6-phosphate isomerase (*Gpi*, EC 5.3.1.9). A discontinuous buffer combination of Tris/HCl (pH 9.0) in the gel and Tris/Glycine (pH 9.0) in the electrophoretic tray was used to resolve peptidases (*Pep*, EC 3.4.11 with leucyl-L-alanine as substrate), phosphoglucomutase (*Pgm*, EC 5.4.2.2), superoxide dismutase (*Sod*, EC 1.15.1.1), and aspartate aminotransferase (*Aat*, EC 2.6.1.1).

Tissue homogenates were also surveyed for variation in non-specific esterases (*Est*, EC 3.1.1. with α-naphtylacetate as substrate) by means of isoelectric focusing (IEF) in precast mini polyacrylamide gels of 50 × 43 × 0.35 mm containing a 4–6.5 pH gradient. IEF gels were run on Pharmacia's LKB PhastSystem (Amersham Biosciences, Belgium) as described by Backeljau et al. (1994). IEF *Est* data were analyzed qualitatively by comparing overall banding patterns. Enzyme staining recipes were adapted from Harris and Hopkinson (1976). Alleles were designated alphabetically according to decreasing electrophoretic mobility (A = fastest allele).

DNA analyses

Of all individuals, total DNA was extracted from a small piece of the foot with the NucleoSpin®Tissue Kit (Macherey–Nagel, Düren, Germany). DNA was used to genotype nine polymorphic microsatellite loci [viz. Rude no 26, 34, 36, 39, 47, 56, 61, 69 and 71; Lance et al. (2010)], as well as to sequence four mtDNA gene fragments [12S rDNA, 16S rDNA, cytochrome oxidase I (COI) and cytochrome B (CytB)], and the two nuclear ribosomal internal transcribed spacers (ITS1 and ITS2), for procedures see Prévot et al. 2013. PCR reactions were performed in a Biometra T-personal Thermal Cycler (Westburg, The Netherlands). Microsatellite electrophoresis and nucleotide sequencing were run on an ABI 3130 × l capillary DNA sequencer (Applied Biosystems, Belgium).

Microsatellite loci were PCR amplified with forward primers that were end labeled with the fluorescent dyes *6-FAM™*, *VIC®*, *PET®* or *NED™*. Primer sequences, repeat motifs and size ranges are given in Lance et al. (2010).

Table 1 Summary of the numbers of specimens and sites sampled by Selander and Hudson (1976) and in this study

Localities	In this study			Selander and Hudson (1976)	
	N	Sites	n	N	n
Botanical garden	2	FmtB1	13 (9/4/0)	5	98 (18/76/4)
		FmtB2	25 (25/0/0)		
Lycée de joffre	1	FmtL	11 (0/11/0)	1	12 (12/0/0)
Protestant cemetery	1	FmtC	20 (0/19/1)	1	32 (6/26/0)
Boulevard des arceaux	2	FmtA1	9 (0/9/0)	24	2 280 (296/1779/205)
		FmtA2	9 (0/9/0)		
Montpellier spot 1	1	FmtS	11 (0/11/0)	n.s	n.s.
Total	7		98 (34/63/1)	32	2,422 (296/1881/209)

n numbers of specimens (dark/light/intermediate), *N* numbers of sites sampled in a locality, *n.s.* not sampled

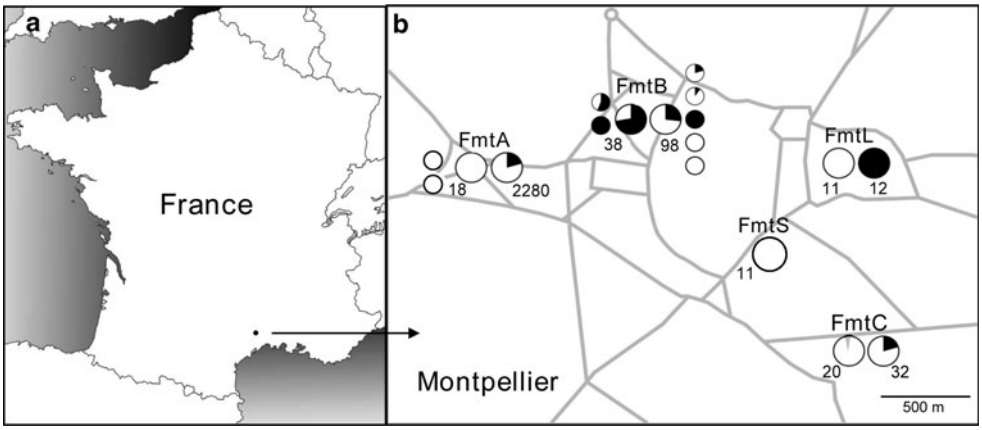

Fig. 2 **a** Geographic location of Montpellier in France. **b** Schematic representation of the distribution and morph composition of the *R. decollata* populations sampled in this study. Circles on the *right hand side* of each pair show the results of Selander and Hudson (1976), circles on the *left hand side* of each pair show our results. *Small circles* morph proportions at each population, *Large circles* morph proportion averaged over all populations at a locality, *White* light morph, *Black* dark morph. Numbers refer to numbers of individuals. *FmtA* Boulevard des Arceaux (FmtA1 and FmtA2), *FmtB* Botanical Garden (FmtB1 and FmtB2), *FmtL* Lycée de Joffre, *FmtC* Protestant Cemetery and *FmtS* Spot 1

Multiplex amplifications were performed in a total volume of 12.5 µl containing 2 × Multiplex PCR Master Mix (HotStarTaq® DNA Polymerase, Multiplex PCR Buffer with 6 mM $MgCl_2$, dNTP Mix; Qiagen, The Netherlands), 2 µM of each primer, 4 µl of sterile RNAse water and 1 µl of DNA. Each PCR run started with an initial step of 15 min at 95 °C, followed by a locus-specific number of cycles involving (1) denaturation for 45 s at 95 °C, (2) annealing for 45 s at a locus-specific temperature, and (3) extension for 1.5 min at 72 °C, and ended with a final extension step of 10 min at 72 °C. Loci Rude26, Rude34 and Rude39 were amplified separately with respectively the following annealing temperatures/number of cycles: 51.4 °C/25 ×, 50.3 °C/25 × and 63 °C/22 ×. Loci Rude36, Rude47, Rude56 and Rude61 were amplified in a multiplex reaction with a primer annealing temperature of 56.6 °C and 25 cycles. Loci Rude69 and Rude71 were amplified simultaneously with a primer annealing temperature of 63.6 °C and 22 cycles. For electrophoresis, 1 µl PCR product was added to 10 µl of a solution containing 5:100 of LIZ 500 in formamide. Specimens with known allele sizes and size standards were included on each gel to ensure scoring accuracy and consistency among gels. Allele sizes were determined with the program GeneMapper v. 4.0 (Applied Biosystems, Belgium).

All the DNA sequences used in this paper were previously established by Prévot et al. (2013), who also described the procedures involved.

Data analysis

Allozyme and microsatellite allele frequencies, heterozygosities [observed: H_{obs}; Nei's (1978) unbiased expected heterozygosities: H_{exp}] and inbreeding coefficients [F_{IS} according to Wright (1978)] were estimated with the program POPGENE v. 1.32 (Yeh et al. 1997). Population differentiation was assessed by pairwise F_{ST} values according to Weir and Cockerham (1984). The significance of F_{ST} was verified with the permutational test (1,000 iterations) implemented in GENETIX v. 4.03 (Belkhir et al. 1996). We calculated pairwise Nm using the relationship $F_{ST} = 1/(4Nm + 1)$ (Wright, 1943). Allele frequency differentiation between the two color morphs was tested with the exact G test implemented by GENEPOP v. 4.1 (Raymond and Rousset 1995). Deviations from Hardy–Weinberg equilibrium (HWE) conditions were tested for each locus and population using the randomization test of F_{IS} (inbreeding coefficient) implemented in FSTAT v. 2.9.3. (Goudet 2001). Selfing rates (S) were calculated using the relationship $S = 2F_{IS}/(1 + F_{IS})$ (e.g. Viard et al. 1997). Deviations from HWE, F_{IS} values and S rates were only assessed in populations with at least nine specimens (arbitrary threshold). Negative S values were set to zero. Null alleles and mis-scoring of microsatellite genotypes may bias F_{IS} estimates upward (Dakin and Avise 2004; David et al. 2007; Jarne and Auld 2006). Therefore, we estimated theoretical mean null allele frequencies (and their standard deviations) with the program FreeNA (Chapuis and Estoup 2007). We also used the program RMES (David et al. 2007; available at http:/ftp.cefe.cnrs.fr) to estimate S, as this approach does not depend on F_{IS} and is supposed to be insensitive to mis-scoring (David et al. 2007). Finally, S was also estimated in RMES using either two-loci heterozygosity disequilibrium (ĝ2) values or a maximum likelihood approach.

All statistical tests were corrected for multiple test biases using the sequential Bonferroni procedure (Rice 1989). Only test values that remained significant after this

correction were considered to be meaningful (e.g. for deciding about HWE deviations) and were used for further calculations (e.g. for inferring Nm from F_{ST}).

DNA sequence divergences between and among morphs are expressed as p-distance using complete deletion, with their standard errors, and were calculated in MEGA v. 4.0 (Tamura et al. 2007). Since the clades A and E_{light} of Prévot et al. (2013) contain haplotypes from several places (Iberian peninsula, France, Tunisia, Malta and Algeria), we re-analyze the DNA data of Prévot et al. (2013) considering only the haplotypes found in Montpellier region.

Results

Color variation

Figure 2 shows the distribution and morph composition of the *R. decollata* populations sampled in this study. The dark morph was only found in FmtB; in FmtB2 all individuals were dark, while in FmtB1 nine dark individuals co-occurred with four light individuals (Table 1). The intermediate specimen was found at FmtC (specimen 341 in Table 2).

Allozymes

Three enzymes did not work (*Lap*, *Mdh* and *Gpi*). Four enzymes (*Aat*, *Pep*, *Sod* and *Pgm*) were monomorphic, yet *Pgd* and *Idh* were polymorphic for two alleles each. All specimens were homozygous at both loci, except for three light specimens that were heterozygous for *Pgd* (specimen 299 from FmtB1, and specimens 407 and 428 from FmtL; Table 2) and three light specimens from FmtC that were heterozygous for *Idh*. Both *Idh* alleles occurred in variable proportions in the two color morphs (Table 3).

Table 2 Atypical marker combinations in two color morphs of *Rumina decollata* in the Montpellier region

Specimen	Site	Morph	Allozyme analysis		Sequence analysis	
			Pgd	*Est*	mtDNA	ITS
299	FmtB1	L	Pgd_A/ Pgd_B	Est_A/ Est_B	L2	ITS_L/ ITS_D
442	FmtB2	D	Pgd_B/ Pgd_B	Est_B/ Est_B	L2	ITS_L
341	FmtC	I	Pgd_B/ Pgd_B	Est_B/ Est_B	D1	ITS_D
342	FmtC	L	Pgd_A/ Pgd_A	Est_A/ Est_A	D1	ITS_D
407	FmtL	L	Pgd_A/ Pgd_B	Est_A/ Est_B	L1	ITS_L
428	FmtL	L	Pgd_A/ Pgd_B	Est_A/ Est_B	L1	ITS_L
429	FmtL	L	Pgd_B/ Pgd_B	Est_B/ Est_B	L1	ITS_L
377	FmtS	L	Pgd_A/ Pgd_A	Est_A/ Est_A	L2	ITS_L/ ITS_D

L light morph, *D* dark morph, *I* intermediate morph

In contrast, the two *Pgd* alleles were nearly diagnostic, since Pgd_A only occurred in the light morph [overall f (Pgd_A) among light specimens = 0.96], whereas the dark morph was fixed for Pgd_B (Table 3). The specimens that compromised the diagnostic character of *Pgd* were the three aforementioned light Pgd_A/Pgd_B heterozygotes, as well as light specimen 429 from FmtL, and intermediate specimen 341 from FmtC, which were homozygous for Pgd_B (Table 2). Hence, in 91/96 (about 95 %) of the specimens, the *Pgd* allele could reliably predict the color phenotype.

Irrespective of whether color morphs were considered together or separately, all sites that were tested for HWE deviations tended to reveal heterozygote deviations from HWE expectations at *Pgd* and *Idh* (Table 3). Yet, none of these heterozygote deviations were significant after Bonferroni correction, except for *Idh* in FmtB1 when both color morphs were combined (Table 3). The mean F_{IS} value at this site was 1.

F_{ST} between all dark specimens together and all light specimens together was 0.78, but mean F_{ST} values between populations within each morph dropped to 0.31 (range: 0.00–0.89) for the light morph (Table 4A) and 0.67 between the two dark populations. The corresponding Nm values were 0.07 between dark and light specimens (overall), 3.6 (range: 0.03–18.45) among light populations (Table 4A) and 0.12 between the two dark populations.

For *Est*, there were two highly diagnostic IEF patterns, for they showed, without exception, pattern Est_A for the light and pattern Est_B for the dark morph (Fig. 3). Both patterns shared four bands, Est_A had six morph specific bands and Est_B had two morph specific bands. The intermediate specimen had an Est_B pattern.

Microsatellites

Summary results for the microsatellite analyses are given in Table 5. Allele frequencies, theoretical null allele frequencies and the *p* values of allele frequency differentiation per color morph are shown in the Online Resource 1. The overall mean null allele frequencies were: 0.191 ± 0.122 in the two populations where both morphs co-occurred, 0.094 ± 0.120 in the light populations, and 0.119 ± 0.130 in the single dark population. The presence of null alleles may be corroborated by the proportion of non-amplifying individuals for several loci (41 % for Rude34, 26 % for Rude71, 11 % for Rude39, 10 % for Rude26, 6 % for Rude56, and 4 % for Rude69).

Table 3 Allozyme data and analysis (*Pgd* and *Idh*)

		FmtB1 All	Light	Dark	FmtB2 Dark	FmtA1 Light	FmtA2 Light	FmtC All	Light	Interm	FmtL Light	FmtS Light
	N	9	4	5	26	9	9	19	18	1	12	12
Pgd												
n:	A	0.389	0.875	–	–	1	1	0.944	1	–	0.833	1
	B	0.611	0.125	1	1	0	–	0.056	–	1	0.167	0
H_{obs}		0.111	0.250	–	–	0	–	0	–	0	0.167	0
H_{exp}		0.503	0.250	–	–	0	–	0.108	0	0	0.289	0
HWE		0.031*						0.028*			0.254	
F_{IS}		0.766						1			0.400	
S		0.867						1			0.571	
Idh												
n:	A	0.667	0.75	0.6	0.038	0	0.222	0.921	0.917	1	0.167	0.083
	B	0.333	0.25	0.4	0.962	1	0.778	0.079	0.083	0	0.833	0.917
H_{obs}		0	0	0	0	0	0	0.158	0.167	0	0	0
H_{exp}		0.471	0.429	0.533	0.075	0	0.366	0.149	0.157	0	0.289	0.159
HWE		0.004*			0.019*		0.012*	1	1		0.006*	0.045*
F_{IS}		1			1		1	−0.086	−0.091		1	1
S		1			1		1	0	0		1	1
Pgd* and *Idh												
H_{obs}		0.016	0.125	0	0	0	0	0.023	0.083	0	0.083	0
H_{exp}		0.139	0.339	0.267	0.038	0	0.183	0.037	0.079	0	0.290	0.080
F_{IS}		0.885			1		1	0.378	−0.051		0.714	1
S		0.939			1		1	0.549	0		0.833	1

N numbers of individuals analyzed, *n* allele frequencies (A and B), H_{obs} observed heterozygosity, H_{exp} Nei's (1978) unbiased expected heterozygosity, *HWE* *p*-values for Hardy–Weinberg equilibrium deviations (significant values for HWE ($p < 0.05$) are marked by *, and are underlined if still significant after sequential Bonferroni correction), F_{IS} inbreeding coefficient (estimated according to Wright 1978). *S* Selfing rate inferred from the classical relationship $S = 2F_{IS}/(1 + F_{IS})$ (Viard et al. 1997). Per site, data are presented for all specimens (both morphs jointly) and per morph. HWE was tested, and F_{IS} and *S* were inferred, only in populations with at least nine individuals

The nine loci yielded 45 alleles, of which 26 (58 %) were shared by both color morphs. Two alleles occurred only in the dark morph and 17 occurred only in the light morph. Yet, the microsatellite data neither showed fixed, morph-specific alleles, nor produced fixed homozygous MLG. Instead they showed substantial numbers of heterozygotes (Table 5).

At sites FmtB1 and FmtC, where the two different morphs co-occurred, there were significant deviations from HWE at 12 out of 14 HWE tests, six of which remained significant after Bonferroni correction. When considering the light morph separately there were significant deviations from HWE at seven out of 23 cases, with two remaining significant after Bonferroni correction, while the same analysis for the dark morph yielded 10 cases out of 15 with significant deviations from HWE, four of which remained so after Bonferroni correction (Table 5). Hence, although H_{obs} for all loci per site were nearly always inferior to H_{exp}, the resulting heterozygote deficiencies were only meaningful in 12 cases (Table 5). The mean F_{IS} values from these 12 sites varied between 0.53 and 1, and *S* values varied between 0.7 and 1. Despite the supposed presence of null alleles, the *S* values calculated with RMES were similar to those derived from F_{IS}, except for FmtA1 and FmtA2 whose *S* values based on RMES where higher, and FmtS of which the RMES based *S* value was lower, than the *S* values calculated from F_{IS} (Table 5).

The overall F_{ST} value between the dark and the light morph was 0.55, but mean F_{ST} values between populations within each color morph were 0.37 (range: 0.07–0.67) for the light morph (Table 4B) and 0.08 for the two dark populations. Yet, this latter value was not significantly different from zero. The corresponding Nm values were 0.13 between dark and light specimens and 0.81 (range: 0.12–3.32) among light populations (Table 4B).

mtDNA and ITS sequence data

The concatenated mtDNA dataset (12S, 16S, COI, CytB) comprised 1,859 bp with 314 variable positions, involving four haplotypes: three for the light color morph [L1, L2 and L3 = haplotypes Eb4, Eb1 and Eb2 from Prévot et al. (2013)] and one for the dark color morph [D1 = haplotype A11 from Prévot et al. (2013)]. The three L haplotypes differed at 1–5 nucleotide positions (mean p-distance of 0.001 ± 0.001), whereas they differed at 328 nucleotide positions (17 of which were indels) from the D haplotype

(mean p-distance of 0.169 ± 0.009). Populations with light specimens comprised one or two L haplotypes (Table 5).

The concatenated ITS sequences (ITS1, ITS2) comprised 1,212 bp with 11 variable positions, involving one haplotype for the light morph (ITS_L) and one for the dark morph (ITS_D). These haplotypes corresponded respectively with the haplotypes nEb2 and nA2 from Prévot et al. (2013). Both haplotypes differed at 33 nucleotide positions, 22 of which were gaps (p-distance of 0.009 ± 0.003). Both haplotypes co-occurred in the sites FmtB1, FmtC and FmtS.

Table 4 Population differentiation in the light morph of *R. decollata* in the Montpellier region

	FmtA1	FmtA2	FmtC	FmtL	FmtS
A					
FmtA1		1.750	0.032	4.585	–
FmtA2	0.125		0.123	–	–
FmtC1	0.888	0.670		0.174	0.058
FmtL1	0.052	0.000	0.590		18.449
FmtS1	0.000	0.000	0.811	0.013	–
B					
FmtA1		0.540	0.184	0.121	0.186
FmtA2	0.317		1.126	0.496	1.404
FmtC1	0.576	0.182		0.295	0.436
FmtL1	0.673	0.335	0.459		3.321
FmtS1	0.573	0.151	0.365	0.070	

Fixation index (*Fst*; below the diagonal) and gene flow (Nm) (above the diagonal) estimates are shown for *Pgd* and *Idh* (A) and microsatellite data (B). Values rounded to the 3rd decimal. Values were calculated for populations with at least 9 specimens. All values remained significant after Bonferroni correction

The concordance between color morph and mtDNA/ITS haplotypes was nearly complete (Tables 3 and 5): of the 63 light specimens, 60 had an L mtDNA haplotype combined with ITS_L, while of the 34 dark specimens, 33 had a D mtDNA haplotype combined with ITS_D. The specimen of the intermediate color morph was also of the latter haplotype combination. There were only two real discrepancies between color phenotype and mtDNA/ITS haplotype, viz. one dark specimen with L haplotypes for mtDNA and ITS (442 in FmtB2) and one light specimen with D haplotypes for mtDNA and ITS (342 in FmtC; Table 2). Two light specimens (299 from FmtB1 and 377 from FmtS) with an L mtDNA haplotype yielded both ITS haplotypes and were assumed to be ITS_L/ITS_D heterozygotes. Hence, the mtDNA haplotype predicted color morph in 96/98 (about 98 %) of the specimens, while ITS and mtDNA/ITS haplotypes did so for 94/98 (about 96 %) of the specimens.

Combined data

In 88 of the 96 specimens (91.7 %) that were scored for all markers, there was a complete correspondence between the color and the molecular phenotypes for *Pgd*, *Est*, mtDNA and ITS. Hence, in these specimens the score of one marker was sufficient to predict the scores of all the other markers. This yielded two main marker combinations: "Light" defined by $Pgd_A + Est_A$ + mtDNA L1-L3 + ITS_L and "Dark" defined by $Pgd_B + Est_B$ + mtDNA D + ITS_D. Yet, eight specimens (8.3 %) showed other marker combinations (Table 2). From these data it appeared that, excluding the specimen with the intermediate morph, color morph was best predicted by mtDNA (about 98 % of

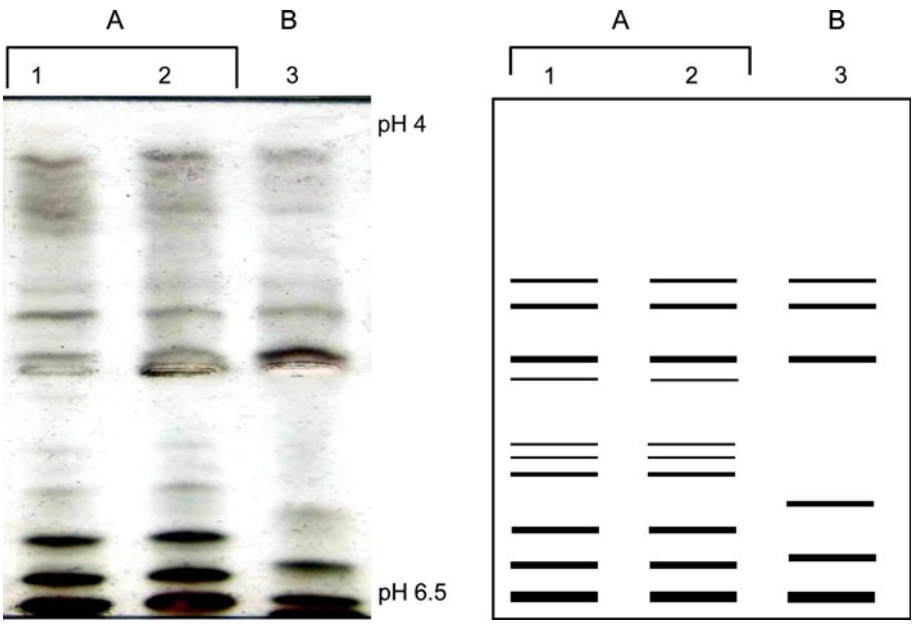

Fig. 3 IEF esterases profiles and their schematic interpretation. *1* light specimen with Pgd_A/Pgd_A, *2* light specimen with Pgd_A/Pgd_B, *3* dark specimen with Pgd_B/Pgd_B

Table 5 Statistical analysis of the microsatellite data

Sites	FmtB1 All			FmtB2 Dark	FmtA1 Light	FmtA2 Light	FmtC All			FmtL Light	FmtS Light
		Light	Dark					Light	Inter		
Rude36											
N	13	4	9	25	9	9	20	19	1	11	11
n	4	2	4	4	2	3	5	5	1	2	2
H_{obs}	0.0769	0	0.1111	0.2000	0.3333	0.4444	0.1500	0.1579		0.0909	0.0909
H_{exp}	0.7046	0.5714	0.6601	0.4384	0.2941	0.3856	0.4295	0.4481		0.0909	0.0909
HWE	0*		0.0003*	0.0003*	1.0000	1.0000	0.0001*	0.0002*		1	1
F_{is}	0.8865		0.8218	0.5345	−0.2000	−0.2203	0.6418	0.6381		−0.0476	−0.0476
S	0.9398		0.9022	0.6966	0	0	0.7818	0.7791		0	0
Rude34											
N	12	4	8	24	2	0	1	1	0	10	9
n	3	3	1	1	1		1	1		1	1
H_{obs}	0	0	0	0	0					0	0
H_{exp}	0.4203	0.7143	0	0	0					0	0
HWE	0.0002*										
F_{is}	1										
S	1										
Rude26											
N	13	4	9	25	9	7	12	12	0	11	11
n	2	2	2	2	1	1	1	1		1	1
H_{obs}	0.0769	0.2500	0	0	0	0	0	0		0	0
H_{exp}	0.4708	0.2500	0.2092	0.0784	0	0	0	0		0	0
HWE	0.0041*		0.0579	0.0203*							
F_{is}	0.8301		1	1							
S	0.9072		1	1							
Rude56											
N	13	4	9	25	8	9	18	17	1	9	10
n	4	4	3	6	2	4	4	4	1	3	5
H_{obs}	0.3846	0.5000	0.3333	0.4000	0.5000	0.3333	0.1667	0.1765		0.4444	0.4000
H_{exp}	0.5815	0.7857	0.4641	0.5388	0.5000	0.7255	0.6651	0.6328		0.5817	0.6684
HWE	0.0686		0.2448	0.0389*		0.0111	0*	0.0001*		0.2449	0.0316*
Fis	0.3122		0.2394	0.2424	−0.0667	0.5135	0.7422	0.7127		0.1910	0.3701
S	0.4758		0.3863	0.3902	0	0.6786	0.8520	0.8323		0.3207	0.5403
Rude61											
N	13	4	9	25	9	9	20	19	1	11	11
n	2	2	2	4	2	4	3	3	1	1	2
H_{obs}	0	0	0	0.0800	0.3333	0.5556	0.2000	0.2105		0	0.0909
H_{exp}	0.3692	0.5714	0.2092	0.3494	0.2941	0.4771	0.3487	0.2845		0	0.0909

Table 5 continued

Sites	FmtB1 All	Light	Dark	FmtB2 Dark	FmtA1 Light	FmtA2 Light	FmtC All	Light	Inter	FmtL Light	FmtS Light
HWE	0.0013*		0.0590	0*	1.0000	1.0000	0.0308*	0.1923			1
F_{IS}	1	1	1	0.7664	−0.2000	−0.2329	0.4118	0.2400			−0.0476
S	1	1	1	0.8678	0	0	0.5834	0.3871			0
Rude47											
N	13	4	9	25	9	9	20	19	1	11	11
n	2	2	2	4	2	3	5	4	1	3	3
H_{obs}	0	0	0	0.0400	0.4444	0.4444	0.4000	0.4211		0.2727	0.6364
H_{exp}	0.3692	0.5714	0.2092	0.2898	0.3660	0.3856	0.5500	0.5021		0.2554	0.6277
HWE	0.0012*		0.0590	0*	1.0000	1.0000	0.0500*	0.2284		1	0.6409
F_{IS}	1	1	1	0.8592	−0.2857	−0.2203	0.2541	0.1388		−0.1186	−0.0621
S	1	1	1	0.9243	0	0	0.4052	0.2438		0	0
Rude69											
N	13	4	9	25	9	9	17	16	1	10	11
n	2	2	2	2	1	1	2	2	1	1	1
H_{obs}	0.0769	0.2500	0	0	0	0	0	0		0	0
H_{exp}	0.4708	0.2500	0.2092	0.0784	0	0	0.2139	0.1210		0	0
HWE	0.0044*		0.0595	0.0212*			0.0029*	0.0323*			
F_{IS}	0.8301	−0.1429	1	1			1	1			
S	0.9072	0	1	1			1	1			
Rude71											
N	6	4	2	12	9	9	15	15	0	10	11
n	2	1	2	2	2	2	1	1		2	2
H_{obs}	0	0	0	0	0	0	0	0		0	0
H_{exp}	0.3030	0	0.6667	0.1594	0.2092	0.3660	0	0		0.3368	0.4156
HWE	0.0910			0.0435*	0.0578	0.0121*				0.0089*	0.0022*
F_{IS}	1		1	1	1	1				1	1
S	1		1	1	1	1				1	1
Rude39											
N	13	4	9	25	9	8	11	11	0	10	11
n	3	2	3	2	1	1	1	1		1	1
H_{obs}	0.0769	0.2500	0	0	0	0	0	0		0	0
H_{exp}	0.5631	0.2500	0.3922	0.0784	0	0	0	0		0	0
HWE	0.0002*		0.0040*	0.0004*							
F_{IS}	0.8579	−0.1429	1	1							
S	0.9235	0	1	1							

Table 5 continued

Sites	FmtB1 All			FmtB2 Dark	FmtA1 Light	FmtA2 Light	FmtC All			FmtL Light	FmtS Light
		Light	Dark					Light	Inter		
All loci											
H_{obs}	0.0769	0.1389	0.0494	0.0800	0.1790	0.2222	0.1019	0.1073	0.000	0.0898	0.1354
H_{exp}	0.4725	0.4405	0.3355	0.2234	0.1848	0.2925	0.2452	0.2209	0.000	0.1405	0.2104
F_{is}	0.8372		0.8527	0.6419	0.0314	0.2403	0.5844	0.5142		0.3608	0.3564
S	0.9114		0.9205	0.7819	0.0609	0.3875	0.7377	0.6792		0.5303	0.5255
$S(g2)$	0.7913		0.8042	0.8472	0.7995	0.7394	0.8806	0.8725		0.7404	0.2461
$S(ML)$	0.6454		0.7140	0.7883	0.7558	0.6708	0.8172	0.8042		0.6740	0
Haplotype											
mt	D1,L2,L3	L2,L3	D1,L2	D1,L2	L2,L3	L2	D1,L1,L2	L1,L2,D1	D1	L1	L2
ITS	L,D,L + D	L,L + D	D	L,D	L	L	L,D	L,D	D	L	L,L + D

N numbers of individuals analyzed, *n* numbers of alleles, H_{obs} observed heterozygosity, H_{exp} Nei's (1978) unbiased expected heterozygosity, *HWE p*-values for Hardy–Weinberg equilibrium deviations (significant values for HWE ($p < 0.05$) are marked by *, and are underlined if still significant after sequential Bonferroni); F_{IS} inbreeding coefficient (estimated according to Wright 1978). *S* Selfing rate deduced from the classical relationship $S = 2F_{IS}/(1 + F_{IS})$ (Viard et al. 1997), and $S(g2)$ and $S(ML)$ calculated by RMES (David et al. 2007). Per site data are presented for all specimens (both morphs jointly) and per morph. HWE was tested, and F_{IS} and *S* were inferred, only in populations with at least nine specimens. Haplotypes for mtDNA and ITS are shown in the two last line of the table

correspondence), followed by ITS, *Est* and *Pgd* all with about 96 % of correspondence.

Discussion

Although the seven enzyme systems surveyed here were also scored by Selander and Hudson (1976), there was little congruence among the locus-specific results of both studies. Based on PAGE we found *Aat*, *Pgm* and *Sod* to be putative single loci, each of which was monomorphic for an allele that was shared by both color morphs. In contrast, using starch gel electrophoresis, Selander and Hudson (1976) reported that each of these enzymes involved 2–5 loci, one or two of which for each of the three enzymes were fixed for different alleles in the two color morphs. Conversely, we found *Idh* to be polymorphic for two alleles shared by both morphs, whereas Selander and Hudson (1976) reported *Idh* to be invariable. So only for *Pep*, *Pgd* and *Est*, our results and those of Selander and Hudson (1976) appear to be somehow congruent, since in both studies *Pep* was invariable, while *Pgd* and *Est* consistently differentiated the two color morphs (despite some observed heterozygotes in *Pgd* and despite the difficulty of comparing individual loci in the complex multi-band *Est* profiles). Irrespective of whether or not the "inconsistencies" between both studies are due to a different resolving power of PAGE vs. starch gel electrophoresis (Geenen et al. 2003), the degree of variation we observed at *Idh* was surprising, since in comparison to Selander and Hudson (1976) and Selander and Ochman (1983), this is the first observation of a variable allozyme locus that neither differentiates the two color morphs, nor corroborates them as fixed homozygous strains. In line with our *Idh* results, but in contrast to Selander and Hudson (1976) and Selander and Ochman (1983), our microsatellite data show even more convincingly that populations and color morphs of *R. decollata* in the Montpellier region do not consist of single or few homozygous MLG. On the contrary, the microsatellite data revealed substantial numbers of heterozygotes, despite the alleged presence of null alleles may have masked heterozygotes. Although the mean null allele frequencies in this study were not exceptional in comparison to other studies (Dakin and Avise 2004), they were not negligible so that most likely we have underestimated the numbers of heterozygotes. This observation and the relatively small number of significant deviations from HWE at the microsatellite loci suggest that outcrossing may be more prevalent in *R. decollata* than indicated by the allozyme data of Selander and Hudson (1976) and Selander and Ochman (1983). These authors relied on an overall mean F_{IS} value of 0.775 to conclude that *R. decollata* mainly reproduces by self-fertilization (Selander and

Hudson 1976). Our overall mean F_{IS} value was of 0.93 for the allozyme data, but only 0.44 for the microsatellite data. Moreover, our F_{IS}, and S values were variable among sites, indicating that the prevalence of selfing may vary among populations. Hence, our data point to a more substantial impact of outcrossing and thus confirm that *R. decollata* has a mixed breeding system. Therefore, *R. decollata* defies the suggestion that hermaphroditic species should be either strict self-fertilizers or strict outcrossers (Goodwillie et al. 2005; Escobar et al. 2011). Yet, this "rule" appears to be challenged by several other terrestrial stylommatophorans, such as *Arion intermedius* (Jordaens et al. unpublished data) and *Carinarion* sp. (Jordaens et al. 2000), *Deroceras laeve* (Nicklas and Hoffman 1981; Foltz et al. 1982).

Obviously, the deep phylogenetic separation of the two color morphs and allozyme MLG of *R. decollata* (Prévot et al. 2013), combined with their highly consistent diagnosability based on their color, *Est* profiles and *Pgd* data, provides a strong corroboration of their status as phylogenetic species.

The present work further suggests that the degree of self-fertilization in *R. decollata* may be much lower than hitherto assumed. In this case, a taxonomic interpretation under the biological species concept (BSC) is allowed. Indeed, three observations indicate that outcrossing does not appear to be exceptional in these snails, viz. (1) the relatively large, and probably still underestimated, numbers of heterozygous individuals, and (2) the occurrence of specimens in which some of the diagnostic markers are incongruent or show mixed combinations (Table 3), and (3) the regular reports of mating couples in *R. decollata* (Batts 1957; Dundee 1986; even if Selander and Ochman (1983) noted that the occurrence of mating behavior on its own is no proof of outcrossing). Anyway, the fact that the strong, multimarker differentiation between the dark and light morph of *R. decollata* is maintained under a mixed breeding system in which outcrossing is not exceptional, suggests that, the two color morphs can also be interpreted as good species under the BSC. The occasional production of intermediary specimens in natural populations (Selander and Ochman 1983; present data) does not invalidate this interpretation, since natural interspecific hybridization between biological species has been reported in many other stylommatophoran taxa, e.g. *Mandarina* spp. (Chiba 2003), *Cerion* spp. (Woodruff and Gould 1987), and *Albinaria* spp. (Giokas et al. 2000). Obviously, the suggestion that the two color morphs of *R. decollata* in the Montpellier area are different biological species needs to be further evaluated in populations where both morphs co-occur. Unfortunately, we had only one such population at hand and this population was too small (FmtB1; Table 1) to make any reliable assessment. However, Selander and Hudson (1976) indicated that both strains tend to preferentially outcross with members of their own strain. Such assortative mating may represent a prezygotic reproductive isolation mechanism that is consistent with a taxonomic interpretation under the BSC (Mayr 1970).

In conclusion, our work confirms that the dark and light color morphs of *R. decollata*, i.e. clades A and Eb in Prévot et al. (2013), are well-supported phylogenetic species, that can be diagnosed by body color, allozyme patterns (*Pgd* and *Est*), and life history differences. We also show that: (1) *R. decollata* has a mixed breeding system, in which outcrossing may be more prevalent than hitherto assumed, and (2) neither populations, nor color morphs consist of single or few MLG, as was previously suggested by, e.g. Selander and Ochman (1983). Finally, the observation that the two color morphs of *R. decollata* correlate with a highly consistent multimarker differentiation in the presence of outcrossing in sympatric conditions, suggests that both morphs may also be interpreted as species under the BSC.

Acknowledgments We are indebted to all the persons who collected specimens and helped us in various ways, as well as to Claúdia Patrão (University of Algarve, Portugal), Dr. Patrick Mardulyn (Free University of Brussels, Belgium) and to the Botanical Garden from the University of Montpellier. V. Prévot was a PhD fellow at the FNRS (Belgium). Financial support was provided by the "Fonds David et Alice Van Buuren" to VP and by BELSPO Action 1 project MO/36/017 to TB. This work was conducted within the framework of the BELSPO IUAP program "SPEEDY" and the FWO research community BeBOL.

References

Backeljau T (1987) Electrophoretic distinction between *Arion hortensis*, *A. distinctus* and *A. owenii* (Mollusca: Pulmonata). Zool Anz 219:33–39

Backeljau T, Breugelmans K, Leirs H, Rodriguez T, Sherbakov D, Sitnikova T, Timmermans JM, Van Goethem JL, Verheyen E (1994) Application of isoelectric focusing in molluscan systematics. The Nautilus 2:156–167

Backeljau T, de Bruyn L, De Wolf H, Jordaens K, Van Dongen S, Winnepenninckx B (1997) Allozyme diversity in slugs of the *Carinarion* complex (Mollusca, Pulmonata). Heredity 78:445–451

Batts JH (1957) Anatomy and life cycle of the snail *Rumina decollata* (Pulmonata: Achatinidae). Southw Nat 2:74–82

Belkhir K, Borsa P, Chikhi L, Raufaste N, Bonhomme F (1996) GENETIX 4.05, logiciel sous WindowsTM pour la génétique des populations. Laboratoire Génome, Populations, Interactions, Université de Montpellier II, Montpellier (France)

Chapuis MP, Estoup A (2007) Microsatellite null alleles and estimation of population differentiation. Mol Biol Evol 24:621–631

Chiba S (2003) Species diversity and conservation of *Mandarina*, an endemic land snail of the Ogasawara Islands. Global Environ Res 7:29–37

Dakin EE, Avise JC (2004) Microsatellite null alleles in parentage analysis. Heredity 93:504–509

David P, Pujol B, Viard F, Castella V, Goudet J (2007) Reliable selfing rate estimates from imperfect population genetic data. Mol Ecol 16:2474–2487

Dundee D (1986) Notes on the habits and anatomy of the introduced land snails, *Rumina* and *Lamellaxis* (Subulinidae). The Nautilus 100:32–37

Escobar JS, Auld JR, Correa AC, Alonso JM, Bony YK, Coutellec M-A, Koene JM, Pointier J-P, Jarne P, David P (2011) Patterns of mating-system evolution in hermaphroditic animals: correlations among selfing rate, inbreeding depression, and the timing of reproduction. Evolution 65:1233–1253

Foltz DW, Schaitkin BM, Selander RK (1982) Gametic disequilibrium in the self-fertilizing slug *Deroceras laeve*. Evolution 36:80–85

Geenen S, Jordaens K, Castilho R, Backeljau T (2003) Congruence between starch gel and polyacrylamide gel electrophoresis in detecting allozyme variation in pulmonate land slugs. Electrophoresis 24:622–627

Geenen S, Jordaens K, Backeljau T (2006) Molecular systematics of the *Carinarion* complex (Mollusca: Gastropoda: Pulmonata): a taxonomic riddle caused by a mixed breeding system. Biol J Linn Soc 89:589–604

Giokas S, Mylonas M, Sotiropoulos K (2000) Gene flow and differential mortality in a contact zone between two *Albinaria* species (Gastropoda; Clausiliidae). Biol J Linn Soc 71:755–770

Goodwillie C, Kalisz S, Eckert CG (2005) The evolutionary enigma of mixed mating systems in plants: occurrence, theoretical explanations, and empirical evidence. Annu Rev Ecol Syst 36:47–79

Goudet J (2001) FSTAT, a program to estimate and test gene diversities and fixation indices (version 2.9.3). Available from http://www2.unil.ch/popgen/softwares/fstat.htm

Harris H, Hopkinson DA (1976) Handbook of enzyme electrophoresis in human genetics. North Holland Publishing Company, Amsterdam

Jarne P, Auld JR (2006) Animals mix it up too: the distribution of self-fertilization among hermaphroditic animals. Evolution 60: 1816–1824

Jordaens K, Geenen S, Reise H, Van Riel P, Verhagen R, Backeljau T (2000) Is there a geographical pattern in the breeding system of a complex of hermaphroditic slugs (Mollusca: Gastropoda: *Carinarion*)? Heredity 85:571–579

Lance SL, Jones KL, Hagen C, Jordaens K, Backeljau T, Prévot V (2010) Fifteen microsatellite loci for the decollate snail, *Rumina decollata*. Conserv Genet Resour 2:287–289

Mayr E (1970) Populations, species, and evolution. Harvard University Press, Cambridge

Nei M (1978) Estimation of average heterozygosity and genetic distance from a small number of individuals. Genetics 89:583–590

Nicklas NL, Hoffman RJ (1981) Apomictic parthenogenesis in a hermaphroditic terrestrial slug, *Deroceras laeve* (Müller). Biol Bull 160:123–135

Prévot V, Jordaens K, Sonet G, Backeljau T (2013) Exploring species level taxonomy and species delimitation methods in the facultatively self-fertilizing land snail genus *Rumina* (Gastropoda: Pulmonata). PLoS ONE 8(4):e60736. doi:10.1371/journal.pone.0060736

Raymond M, Rousset F (1995) GENEPOP (version 1.2): population genetics software for exact tests and ecumenicism. J Hered 86:248–249

Rice WR (1989) Analyzing tables of statistical tests. Evolution 43:223–225

Selander RK, Hudson RO (1976) Animal population structure under close inbreeding: the land snail *Rumina* in southern France. Am Nat 110:695–718

Selander RK, Kaufman DW (1973) Self-fertilization and genetic population structure in a colonizing land snail. Proc Natl Acad Sci USA 70:1186–1190

Selander RK, Ochman H (1983) The genetic structure of populations as illustrated by molluscs. Isozymes: Curr Top Biol Med Res 10: Genet Evol: 93–123

Selander RK, Kaufman DW, Ralin RS (1974) Self-fertilization in the terrestrial snail *Rumina decollata*. The Veliger 16:265–270

Tamura K, Dudley J, Nei M, Kumar S (2007) MEGA4: molecular evolutionary genetics analysis (MEGA) software version 4.0. Mol Biol Evol 24:1596–1599

Viard F, Justy F, Jarne P (1997) The influence of self-fertilization and population dynamics on the genetic structure of subdivided populations: a case study using microsatellite markers in the freshwater snail *Bulinus truncatus*. Evolution 51:1518–1528

Weir BS, Cockerham CC (1984) Estimating F-statistics for the analysis of population structure. Evolution 38:1358–1370

Woodruff DS, Gould SJ (1987) Fifty years of interspecific hybridization: genetics and morphometrics of a controlled experiment involving the land snail *Cerion* in Florida. Evolution 41:1022–1045

Wright S (1943) Isolation by distance. Genetics 28:114–138

Wright S (1978) Evolution and the genetics of populations. University of Chicago Press, Chicago

Yeh FC, Yang R-C, Boyle TBJ, Ye Z-H, Mao XJ (1997) POPGENE, the user-friendly shareware for population genetic analysis. University of Alberta, Canada, Molecular Biology and Biotechnology Centre